Modeling Liver with Glisson's Capsule in Real-Time Medical Simulations

Tomáš Golembiovský*
Faculty of Informatics
Masaryk University
Brno, Czech Republic

Igor Peterlík
Institut Hospitalo-Universitaire
Strasbourg, France

Christian Duriez
INRIA
Lille, France

Stéphane Cotin
INRIA
Lille, France

Abstract

The accurate mechanical modeling of liver is of a paramount interest in simulation-based operation planning and computer-aided per-operative guidance. However, the realistic simulation of liver behaviour is a challenging task, since the organ is composed of three constituents: parenchyma, vascularization and Glisson's capsule, each having different mechanical properties.

While a real-time simulation of vascularized liver has been already described in [Peterlík et al. 2012], the Glisson's capsule has not been included in the modeling. In [Hollenstein et al. 2006; Ahn and Kim 2010] it is shown that the capsule plays an important role mainly in the vicinity of the surgical tools. Therefore, the accuracy of the liver response in the vicinity of the surgical tool requires correct modeling of the capsule as a component of the liver model.

The measures performed on the capsule report stiffness which is significantly higher than that of the parenchyma, however, the thickness of the membrane does not exceed 100μm. For this reason, it is not possible to model the capsule with standard volume elements usually employed for the parenchyma. In our approach, we rely of corotational membrane elements based on constant-strain formulation, which are coupled mechanically to the underlying tetrahedra. We show that using this model we are able to reproduce the experiments reported in [Hollenstein et al. 2006], while maintaining the real-time aspect of the simulation.

CR Categories: I.6.5 [Simulation and Modeling]: Model Development— [J.3]: Life and Medical Sciences—Health;

Keywords: deformable liver model, Glisson's capsule

*nyoxi@ics.muni.cz

1 Introduction

According to the statistics, nearly 100,000 European citizens die of cirrhosis or liver cancer each year. Although new methods such as radio-frequency- and cryo-ablation known in the interventional radiology seem to be promising, surgery remains the option that offers the foremost success rate against these pathologies. Nevertheless, surgery is not always performed due to several limitations, in particular the determination of accurate eligibility criteria for the patient. In this context, the pre-operational planning becomes a crucial task having a significant impact on the treatment.

Computer-aided physics-based medical simulation has proven to be an extremely useful technique in the area of medical training. Nevertheless, whereas generic models are usually required in training simulators, accurate patient-specific modeling becomes necessary as soon as computer simulation is to be employed in the preoperative planning. At the same time, interactivity of such models remains an important aspect, requiring real-time simulation which is often difficult to achieve given the complexity of soft tissues.

When simulating the behavior of human liver, the task of real-time accurate modeling is challenging, mainly because of the complex structure of this organ composed of three main constituents: *parenchyma*, *vascular networks* and *Glisson's capsule*. The parenchyma has certainly been the most studied component of the liver; actually researchers agree on hyperelastic properties of the tissue, for which the mechanical parameters have been reported for example in [Kerdok et al. 2006; Gao et al. 2009]. Moreover, several methods have been proposed to model the hyperelastic behaviour at real-time rates, such as multiplicative Jacobian decomposition introduced in [Marchesseau et al. 2010].

The mechanical importance of the vascular structures in liver is studied in [Peterlík et al. 2012]. It shows that the influence of vessels on the mechanical behaviour of the organ is significant. Since a detailed modeling of the vessels would be extremely costly (mainly because of the small thickness of the vessel wall), the authors propose a composite model allowing for real-time simulation.

Rather a small number of studies have been conducted dealing with the third liver constituent, the Glisson's capsule. Quantitative results of experiments on a porcine liver have been published in [Umale et al. 2011]; the measurements indicate that although being very thin (10–$20\mu m$), the capsule shows to be stiff in tensile tests: the Young's modulus of the capsule reported to be 8.22 ± 3.42 MPa exceeds the values for the parenchyma by three orders of magnitude. This suggests that the mechanical influence of the membrane on the liver behaviour is not negligible.

In [Hollenstein et al. 2006], a local influence of the capsule has been measured using a special aspiration device. The study was then repeated in vivo on human patients during the operation, confirming the mechanical importance of the membrane [Ahn and Kim 2010; Nava et al. 2008].

In this paper we present preliminary results of our work on the complete liver model. We present a real-time composite model accounting for parenchyma and Glisson's capsule. The model is based on two different finite element representations for each con-

stituent coupled together. We show that the model mimics the *local* experiments described in [Hollenstein et al. 2006].

The paper is organized as follows: first we describe the proposed model of liver with capsule. Second, we validate our model in context of local deformations by reproducing the aspiration test described in [Hollenstein et al. 2006]. We conclude by summarizing future steps towards the complete liver model.

2 Model

In this section we describe the construction of a composite model based on two components: tetrahedral FE model of the parenchyma and triangular membrane elements used for the capsule.

2.1 Parenchyma

It is known that the parenchyma exhibits non-linear viscoelastic behaviour [Marchesseau et al. 2010]. However, as we are mainly interested in the static equilibrium, we do not model the time-dependent phenomena related to viscosity.

The parenchyma is modeled using corotational finite elements [Felippa and Haugen 2005]. Although it relies on linear stress-strain relationship, large displacements including rotations are modeled correctly. While in the full non-linear formulation the stiffness matrix relates the forces $\mathbf{f}$ and displacements $\mathbf{u}$ as $\mathbf{f} = K(\mathbf{u})$, the corotational model requires the stiffness matrix $\mathbf{K}_0$ of the system to be computed only once before the simulation begins. Then, in each step, the motion of each element e is decomposed into rigid rotation $\mathbf{R}^e$ and local deformation. The rotations are then used to update each local element stiffness matrix as $\mathbf{R}^e\mathbf{K}_0\mathbf{R}^{e\top}$ whereas the deformations are used to compute the linear strain in the local corotational frame. There are several ways of computing the corotational frame for elements; we rely on the geometrical method proposed in [Nesme et al. 2005].

2.2 Glisson's Capsule

The thickness of the Glisson's capsule is relatively small: the values in range of 10-20 μm have been reported in [Umale et al. 2011]. It is not possible to model such thin structure with classical tetrahedral elements, if the real-time aspect of the simulation is to be preserved. Furthermore, modeling both the tissue and the capsule would require an extremely dense mesh to avoid numerical instabilities and thus would significantly violate the speed requirements imposed for medical simulators. Instead, modeling the capsule with two-dimensional elements that abstract from the thickness in the third dimension seems to be a natural choice. In the elasticity theory, this functionality is usually provided by membrane and shell elements. Based on the observation of its behaviour, we also assume negligible bending forces and propose a model based on membrane elements. To maintain simplicity of the composite model we choose simple triangular elements with constant strain (CST).

The computation of elastic stiffness matrix follows the common derivation

$$\mathbf{K}^m = \int_V \mathbf{B}^T\mathbf{E}\mathbf{B}dV \quad (1)$$

$$= h\int_A \mathbf{B}^T\mathbf{E}\mathbf{B}dA \quad (2)$$

$$= hA\mathbf{B}^T\mathbf{E}\mathbf{B} \quad (3)$$

where $\mathbf{B}$ is the strain-displacement matrix, $\mathbf{E}$ the material matrix, h is the thickness and A area of the element. In the previous (2) follows from the fact that we assume constant thickness of the element and (3) follows from the fact that the strain-displacement matrix is constant in our case. The strain-displacement matrix for the CST element can be expressed as:

$$\mathbf{B} = \frac{1}{2A}\begin{bmatrix} y_{23} & 0 & y_{31} & 0 & y_{12} & 0 \\ 0 & x_{32} & 0 & x_{13} & 0 & x_{21} \\ x_{32} & y_{23} & x_{13} & y_{31} & x_{21} & y_{12} \end{bmatrix} \quad (4)$$

The values $x_{ij} = x_i - x_j$ and $y_{ij} = y_i - y_j$ are computed from the x or y coordinates of the nodes i, j of the triangular element. The reader can refer to the respective literature [Felippa 2003] for more thorough description.

Similarly as with model of parenchyma we use linear elastic material and employ the corotational formulation for the CST elements.

2.3 Coupling Between Capsule and Parenchyma

The literature reports high cohesion between capsule and parenchyma. Based on this property we assume there is no relative motion of the capsule w. r. t. the parenchyma. Although an arbitrary surface mesh could be used to model the capsule, we exploit the fact that the parenchyma is modeled by tetrahedral elements having triangular faces. Thus, as the boundary of the volumetric mesh is already triangulated, we simply employ the triangles on the mesh surface to model the capsule.

Using directly the boundary of the tetrahedral mesh does not only solve the problem of building the surface mesh, but has one more advantage: the nodes of the triangular mesh coincide with the nodes of the tetrahedral mesh, so no projection of one mesh onto the other is needed. Moreover, the stiffness matrices for capsule and parenchyma are then easily assembled together. Without the loss of generality we can assume the tetrahedron consists of nodes p_1, p_2, p_3 and p_4 and the boundary triangle has nodes p_1, p_2 and p_3. We can reorder the degrees of freedom so that the stiffness matrix $\mathbf{K}^t$ for the tetrahedron can be written as:

$$\mathbf{K}^t = \left[\begin{array}{c|c} \mathbf{K}^t_{1-3,1-3} & \mathbf{K}^t_{1-3,4} \\ \hline \mathbf{K}^t_{4,1-3} & \mathbf{K}^t_{4,4} \\ \cdot & \end{array}\right] \quad (5)$$

Hence, the assembled stiffness matrix for the element is

$$\mathbf{K} = \left[\begin{array}{c|c} \mathbf{K}^t_{1-3,1-3} & \mathbf{K}^t_{1-3,4} \\ \hline \mathbf{K}^t_{4,1-3} & \mathbf{K}^t_{4,4} \end{array}\right] + \left[\begin{array}{c|c} \mathbf{K}^m & 0 \\ \hline 0 & 0 \end{array}\right] \quad (6)$$

where $\mathbf{K}^m$ is the stiffness matrix of the triangular membrane.

The resulting system of linear equations is solved by direct solver based on Cholesky decomposition.

3 Methods

The model presented in the previous section was implemented in SOFA[1] and a set of numerical simulations was performed. In this section we provide comparison of local deformations with the results reported in literature to validate the method.

During the contact with an instrument such as probe, needle, scalpel and others, specific deformations take place in the vicinity of the instrument. This type of deformation may not necessarily induce the deformation of the object as a whole and therefore can be considered as local. Correct material properties are not only important to quantify the displacement, but also play an important role in capturing the correct area of the deformation or its profile near the instrument.

A good example of such a local deformation is the aspiration test where the response of liver exposed locally to a negative pressure is

[1] www.sofa-framework.org

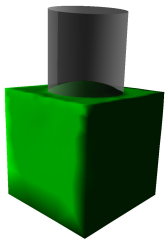

Figure 1: *The SOFA simulation scene of the aspiration test.*

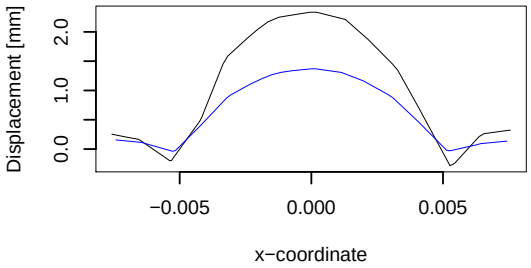

Figure 2: *Displacement profile of the cube in the aspiration test with (blue) and without (black) the capsule.*

measured. The aspiration device consists of a tube having 1 cm in diameter and allows to control the pressure inside the tube. The test is performed by attaching the tube to the tissue and measuring the tissue response. We set up a simulation in SOFA to reproduce the experiment (see Fig. 1): we meshed a $15\times15\times15\,\text{mm}^3$ cube representing the tissue resulting in 2648 tetrahedra. Then we attached a 1 cm tube and applied a pressure of 3 kPa inside the tube.

Since the tube is in direct contact with the tissue, uni-lateral constraints with friction were chosen to model this interaction properly. We opted for a method based on *non-linear complementarity problem* (NLCP) where the non-linearity is introduced due to the friction. The NLCP allows for solution of the Signorini's problem to avoid any interpenetration between the colliding objects (see [Duriez et al. 2006] for details). Since NLCP requires explicitly the computation of compliance matrix which is homogeneous to the inverse of the stiffness matrix, we employed a direct solver based on LDL decomposition to solve the system and compute the inverse matrices.

4 Results and Discussion

As the first step, we evaluate the influence of the Glisson's capsule on the mechanical response of the tissue during the aspiration test. In [Hollenstein et al. 2006] it is reported that the influence of the capsule is significant, as modeling only the parenchyma without considering the membrane results in overestimation of the deformation by a factor of 2 to 3. In order to verify this observation, we performed a simulation using capsule parameters measured experimentally on ex-vivo pig liver [Umale et al. 2011]: Young's modulus of the membrane was set to E_c=8.22 MPa and thickness was t_c=20 μm. Since the values for parenchyma elasticity reported in the literature vary significantly being usually reported between 2 kPa to 5 kPa, we employed a value E_p=3.5 kPa for the Young's modulus of the parenchyma.

In Fig. 2 the profiles of cuts in the middle of the test cube are presented showing significantly larger deformation in the model without capsule assuming that the same negative pressure was applied on the tissue surface inside the tube. Moreover, it can be observed

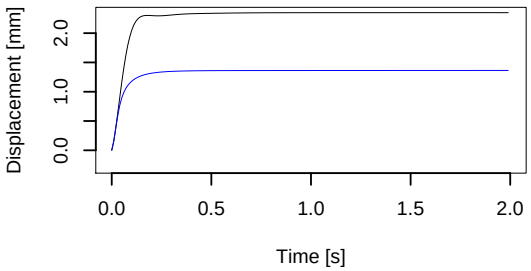

Figure 3: *Evolution of the displacement at the center in time for test with (blue) and without (black) the capsule.*

that the deformation without capsule is overestimated by a factor close to 2, which is in perfect agreement with the results reported in [Hollenstein et al. 2006]. Fig. 3 presents the evolution of displacement in time at central node on the cube surface. The effect of increased combined stiffness is clearly visible.

In the second step, we employed the simulation to reproduce the displacements values obtained via simulation in [Hollenstein et al. 2006; Nava et al. 2008]. Whereas the simulation in the referenced work was done on a mesh composed of tetrahedral elements for both the parenchyma and the capsule, we modeled the capsule using the triangular elements as shown in section 2.2.

Since the Young's moduli of neither parenchyma (E_p) nor capsule (E_c) were specified exactly, we obtained both as follows: first, we performed a set of simulations without the capsule for different values of E_p: the value that provided a good match with reported displacements was E_p=30 kPa. Then, we fixed the thickness of the capsule to be t=93 μm (reported as the average value in the paper) and using E_p=30 kPa, we ran the simulation repeatedly using the model with the capsule. In each simulation we used different value E_c of the Young's modulus for the capsule in order to minimize the displacement error w.r.t. the reported values. The minimal value of error (not exceeding 1%) was obtained for E_c=3 MPa. This value lies in the range of capsule elasticity coefficients reported by experimental measurements.

In the scenario presented in this paper, we focus on local influence of the capsule. Nevertheless, it is possible to employ the actual model to demonstrate the global impact of the capsule and to further validate the accuracy of such a complete model w.r.t. experimental measures. Detailed description of such validation is however beyond the scope of this paper. In spite of this we would like to emphasize that we have already integrated the capsule model with vascularized liver model described in [Peterlík et al. 2012]. Adding the capsule did not affect the performance significantly: a visual refresh rate exceeding 25 FPS was achieved on a PC with CPU Intel i7 running at 3.00 GHz. This suggests that the proposed technique is compatible with real-time simulation of whole organ while modeling the local properties accurately.

5 Conclusions and Future Work

In the paper we presented a model of tissue with capsule based on two separated models for parenchyma (corotational tetrahedral elements) and membrane (CST triangular elements). Employing a simulation scenario known as aspiration test, we compared the model with experimental data provided in the literature and verified the results obtained in the simulation w.r.t. to a standard computationally expensive model based entirely on volume elements [Hollenstein et al. 2006]. We obtained values which were in good correspondence with results reported in the literature.

Presently we are focusing on the validation of the model also in

context of global deformations of the organ where we believe the capsule plays an essential role as well. This task is however complicated due to the limited number of experimental studies dealing with both the parenchyma and the capsule.

References

AHN, B., AND KIM, J. 2010. Measurement and characterization of soft tissue behavior with surface deformation and force response under large deformations. *Medical Image Analysis 14*, 2, 138–148.

DURIEZ, C., DUBOIS, F., KHEDDAR, A., AND ANDRIOT, C. 2006. Realistic haptic rendering of interacting deformable objects in virtual environments. *IEEE Transactions on Visualization and Computer Graphics 12*, 1, 36–47.

FELIPPA, C., AND HAUGEN, B. 2005. A unified formulation of small-strain corotational finite elements: I. theory. *CMAME 194*, 21-24, 2285–2335.

FELIPPA, C. A. 2003. A study of optimal membrane triangles with drilling freedoms. *CMAME 192*, 16-18, 2125–2168.

GAO, Z., KIM, T., JAMES, D., AND DESAI, J. 2009. Semi-automated soft-tissue acquisition and modeling for surgical simulation. In *Automation Science and Engineering*.

HOLLENSTEIN, M., NAVA, A., VALTORTA, D., SNEDEKER, J. G., AND MAZZA, E. 2006. Mechanical characterization of the liver capsule and parenchyma. In *Biomedical Simulation*, vol. 4072 of *LNCS*. Springer Berlin Heidelberg, 150–158.

KERDOK, A. E., OTTENSMEYER, M. P., AND HOWE, R. D. 2006. Effects of perfusion on the viscoelastic characteristics of liver. *Journal of Biomechanics 39*, 12, 2221–2231.

MARCHESSEAU, S., HEIMANN, T., CHATELIN, S., WILLINGER, R., AND DELINGETTE, H. 2010. Multiplicative jacobian energy decomposition method for fast porous visco-hyperelastic soft tissue model. In *MICCAI 2010*, vol. 6361 of *LNCS*. 235–242.

NAVA, A., MAZZA, E., FURRER, M., VILLIGER, P., AND REINHART, W. 2008. In vivo mechanical characterization of human liver. *Medical Image Analysis 12*, 2, 203–216.

NESME, M., PAYAN, Y., AND FAURE, F. 2005. Efficient, physically plausible finite elements. In *Eurographics (short papers)*, J. Dingliana and F. Ganovelli, Eds.

PETERLÍK, I., DURIEZ, C., AND COTIN, S. 2012. Modeling and real-time simulation of a vascularized liver tissue. In *MICCAI 2012*, vol. 7510 of *LNCS*, 50–57.

UMALE, S., CHATELIN, S., BOURDET, N., DECK, C., DIANA, M., DHUMANE, P., SOLER, L., MARESCAUX, J., AND WILLINGER, R. 2011. Experimental in vitro mechanical characterization of porcine glisson's capsule and hepatic veins. *Journal of Biomechanics 44*, 9.